

Cite this article as: Luo Hongbo, Lü Yanjun, Zhao Xiaowei, et al. Tribological Performance and Evolution Characteristics of WC Coating During Nano-scratching: a Molecular Dynamics Study[J]. Rare Metal Materials and Engineering, 2023, 52(09): 3037-3046.

ARTICLE

Tribological Performance and Evolution Characteristics of WC Coating During Nano-scratching: a Molecular Dynamics Study

Luo Hongbo¹, Lü Yanjun¹, Zhao Xiaowei¹, Zhang Yongfang²

¹ School of Mechanical and Precision Instrument Engineering, Xi'an University of Technology, Xi'an 710048, China; ² Faculty of Printing, Packaging Engineering and Digital Media Technology, Xi'an University of Technology, Xi'an 710048, China

Abstract: In order to investigate the nano-friction evolution characteristics of WC coating during the nano-scratching process, the molecular dynamics simulation model was established under different conditions (load, scratching-depth, scratching-velocity) by the large-scale atomic /molecular massively-parallel simulator. Results show that the friction force and coefficient of friction are increased with increasing the scratching depth. When the indenter scratches the specimen, the atoms are squeezed, sheared, and piled up in front of the indenter and at both sides of the groove along scratching direction. The instantaneous friction curve presents the distinct tribological characteristics during the initial and stable stages, and the dislocation, slip, interstitial, or vacancy occurs in the region under the indenter during the friction process. With increasing the scratching velocity, the strain energy of system exceeds the bonding energy caused by interatomic constraint. The atoms break the constraint and are stacked on both sides of the scratching grooves. Additionally, the surface morphology and the outer edge of accumulated atoms become rough, and defects appear in the subsurface crystal structure. This research provided the microscopic wear mechanism of WC coating at nano-scale during friction process.

Key words: WC coating; nano-scratching; molecular dynamic simulation; friction force; coefficient of friction; morphology

The performance of coating material has significant impact on the service security and service lifetime of equipment. It is estimated that nearly two thirds of coating materials for engineering components suffer from severe wear and friction failure^[1]. Therefore, it is of great significance to improve the friction performance of coating materials^[2]. The wear-resistant coating has been widely applied on the surface of motion pair, particularly in the miniaturized precision parts, which requires the investigation on tribological performance at micro-scale^[3]. Therefore, the comprehensive investigation of the tribological behavior at micro- and nano-scale is important for the design of coating materials.

Since its good compactness, fine impact resistance, high toughness, good wear resistance, and high hardness, tungsten carbide (WC) coating can effectively improve the wear resistance of mechanical parts. Hence, WC coating is widely used in machinery, aviation, aerospace, and other fields^[4-5].

However, many factors lead to the low interfacial bonding strength between WC coating and matrix, which restricts the large-scale production and application of WC coating. Recently, the tribological performance of WC coating has been extensively researched. Sun et al^[6] prepared WC-based coating through electric contact strengthening (ECS) method, and the effects of ESC processing duration on the morphology, element distribution, hardness, and phase composition of surfaces were investigated. Xiao et al^[7] investigated the phase composition, microstructure, microhardness, friction, and wear properties of the Fe-WC composite coatings. The thermal damage forms caused by WC particles and the influence mechanism of the microstructure evolution and wear performance are discussed. The fracture and crack propagation behavior of WC-Co cemented carbides are studied under different loads^[8-10]. Generally, the powder ratio, preparation technique, and mechanical properties of WC

Received date: November 15, 2022

Foundation item: National Natural Science Foundation of China (52075438); Key Research and Development Program of Shaanxi Province (2020GY-106); Open Project of State Key Laboratory for Manufacturing Systems Engineering (sklms2020010)

Corresponding author: Lü Yanjun, Ph. D., Professor, School of Mechanical and Precision Instrument Engineering, Xi'an University of Technology, Xi'an 710048, P. R. China, E-mail: yanjunlu@xaut.edu.cn

Copyright © 2023, Northwest Institute for Nonferrous Metal Research. Published by Science Press. All rights reserved.

coating materials have been analyzed. However, the evolution process of tribological properties at nano-scale is rarely studied, especially the atom behavior during service process, and the anti-friction and anti-wear mechanisms of WC coating at atomic-scale is still obscure.

Molecular dynamics (MD) simulations attract much attention as an efficient method to investigate the local contact and friction behavior at the micro-scale by nano-indentation and nano-scratches^[11-13]. Anil et al^[14] conducted common neighbor analysis of Cu-Ni based on the dislocation mechanism, and the effects of size, indenter velocity, and thickness of nano-coating on hardness and dislocations were investigated by MD method. Singh et al^[15] simulated the sintering process of WC nanocrystalline particles at micro-scale by MD method, studied the tensile strength during the sintering process at different temperatures, and found the optimal sintering parameters for WC powder at nano-scale. Xu et al^[16] investigated the effects of texture shape, texture spacing, and indenter size on the force, temperature, and plastic deformation of nano-textured silicon surfaces during friction process by MD simulation. The friction mechanism of nano-texture is revealed, which is beneficial to design micro/nano-devices. Feng et al^[17] discussed the deformation and plasticity mechanisms of WC, Co, and WC-Co composites by MD simulations at atomic-scale. It is found that the nucleation, expansion, and interaction of dislocations are obviously dependent on the loading direction. MD simulation is an effective method to reveal the nano-scale tribological properties and micro-damage. The atomic-scale mechanical response and behavior of the crystal structures can also be studied through MD simulations. The nano-scratching process can produce the atomic-scale friction, which is beneficial to the investigation of interactions between matrix surface and abrasive atoms. Besides, this is also an ideal method to study the tribological performance of thin film coatings at nano-scale^[18-19].

In this research, the tribological properties of WC coating at atomic-scale were investigated based on MD theory and computer simulation. In the nano-scratching process, the Tersoff three-body potential function was used to characterize the interactions among atoms, and the friction process of WC coating was simulated under different conditions of scratching-depth, load, and scratching velocity. The tribological characteristics and evolution of WC coating were analyzed based on the friction force, coefficient of friction (COF), and wear morphology. This research provided theoretical support to improve the mechanical properties of WC coating and to reveal the friction failure mechanism at nano-scale.

1 Experiment and Simulation

1.1 Model geometry and computational details

The single crystal cell structure of WC coating is shown in Fig. 1. Fig. 2 shows the calculation model of WC coating, which is the expansion model from WC crystal cell. A large-scale atomic/molecular massively-parallel simulator^[20] was used to conduct MD simulation in this research, and the open visualization tool was used to obtain the atomic snapshots and

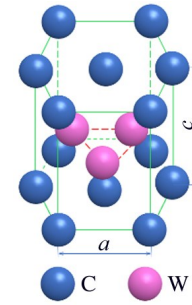


Fig.1 Schematic diagram of WC crystal cell model

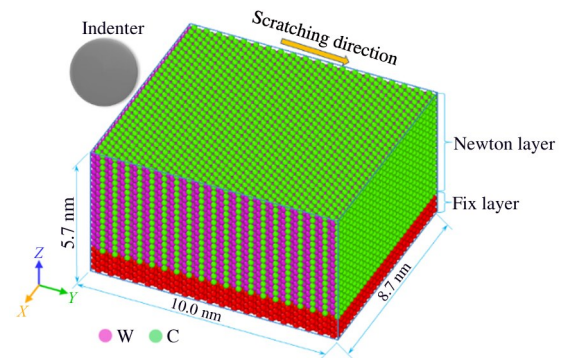


Fig.2 Schematic diagram of nano-scratching simulation model

to analyze the simulation data^[21].

WC crystal cell has hexagonal close-packed (hcp) structure. The normal c/a ratio of hcp structure is 1.633, but the lattice constants of WC cell are $a=b=0.29$ nm, $c=0.2831$ nm, suggesting that the c/a ratio is 0.973, which is much lower than the normal hcp ratio. The a_1 , a_2 , a_3 , and c hcp crystal directions of WC cell are $[2\bar{1}\bar{1}0]$, $[\bar{1}2\bar{1}0]$, $[\bar{1}\bar{1}20]$, and $[0001]$, respectively. Through the initial modeling software AtomsK, an orthogonal cell equivalent to the orthogonal hexagonal lattice was obtained, and the X , Y and Z directions are parallel to the lattice orientations of $[\bar{1}2\bar{1}0]$, $[10\bar{1}0]$, and $[0001]$, respectively. After model expansion, the size of WC simulation model was $17a \times 15b \times 25c$, which consisted of 15 000 atoms. In order to avoid the influence of elastic deformation of indenter which was regarded as rigid bodies with relatively fixed positions of internal atoms, and to prevent deformation and wear during the whole scratching process, the scratching direction of the model was along the Y -axis. The simulation parameters of WC coating model during nano-scratching process are shown in Table 1. The atom layer at the model bottom was set as a fixed layer to provide rigid support, and other atom layers were set as the Newton layer.

In the simulation, X and Y directions were set as periodic boundary conditions to reduce the influence of model scale on the simulation results; the free boundary conditions were applied to the Z direction; the simulation time step was set as 0.1 fs; the atomic motion equation was solved by the Velocity-Verlet algorithm. NVT ensemble and Langevin temperature control method were used to keep the system temperature at

Table 1 MD simulation parameters of WC coating model during nano-scratching process

Parameter	WC	Rigid indenter
Dimension	8.7 nm×10.0 nm×5.7 nm	R=1.5 nm
Number of atoms	15 000	-
Interatomic potential	Tersoff	-
Time step/fs	0.1	-
Initial temperature/K	300	-
Scratching velocity/m·s ⁻¹	-	200, 400, 800
Normal load/nN	-	0.8, 8, 80
Scratching depth/nm	-	0.4, 0.9, 1.4

around 300 K during the nano-scratching process^[22].

1.2 Interatomic potential

MD method has obvious advantages in simulation and prediction of the material properties at micro- and nano-scale. The atomic motion at nano-scale obeys the Newton laws in MD simulations^[23-24]. Therefore, for an independent system consisting of N particles, the equation of motion particles can be described as follows:

$$a_i = \frac{d^2 r_i}{dt^2} = \frac{F_i + f_i}{m_i} \quad (1)$$

$$F_i = -\nabla_i U \quad (2)$$

where m_i denotes the mass of i atom; r_i denotes the position of i atom; F_i denotes the interatomic interaction force of i atom; f_i indicates other forces of i atom; U is the total potential energy of the system.

The three-body potential energy function was used to describe the interatomic interactions, and its accuracy determined the reliability of the simulation results. Hence, the accuracy of potential function is important to MD simulation. Because the interaction mechanism of WC coating is very complex, the interactions of atoms for a single potential function could not be accurately characterized. Therefore, the three-body Tersoff empirical potential was used to characterize the interatomic actions of WC coating based on the bonding order^[25], which was particularly suitable to describe the interactions between C and W atoms bonded by covalent bonds. The interatomic potential energy of two adjacent atoms i and j can be expressed as follows:

$$E = \sum_i E_i = \frac{1}{2} \sum_{i \neq j} V_{ij} \quad (3)$$

$$V_{ij} = f_C(r_{ij}) [f_R(r_{ij}) + b_{ij} f_A(r_{ij})] \quad (4)$$

$$f_C(r) = \begin{cases} 1 & r < R - D \\ \frac{1}{2} - \frac{1}{2} \sin\left(\frac{\pi}{2} \frac{r - R}{D}\right) & R - D < r < R + D \\ 0 & r > R + D \end{cases} \quad (5)$$

$$f_R(r) = A \exp(-\lambda_1 r) \quad (6)$$

$$f_A(r) = -B \exp(-\lambda_2 r) \quad (7)$$

$$b_{ij} = (1 + \beta^n \zeta_{ij}^n)^{-\frac{1}{2n}} \quad (8)$$

$$\zeta_{ij}^n = \sum_{k \neq i, j} f_C(r_{ik} + \delta) g[\theta_{ijk}(r_{ij}, r_{ik})] \exp[\lambda_3^m (r_{ij} - r_{ik})^m] \quad (9)$$

$$g(\theta) = r_{ijk} \left[1 + \frac{c^2}{d^2} - \frac{c^2}{d^2 + (\cos \theta - \cos \theta_0)^2} \right] \quad (10)$$

where E denotes the total energy of the system; the subscripted parameters i, j , and k represent different atoms in the system; r_{ij} is the length of ij bond; θ_{ijk} indicates the bond angle between ij and ik bonds; b_{ij} denotes the bond order function and reflects the saturation state of the covalent bond; V_{ij} indicates the interaction neighboring atoms; f_R and f_A denote the repulsive term and attractive term between the atoms, respectively; f_C is a smooth truncation function; ζ indicates the effective coordination number; $g(\theta)$ is the function of bond angle; the detailed descriptions of the other parameters are reported in Ref.[26-27].

In the simulation of nano-scratching process of WC coating, three kinds of interatomic interactions, including the W-W interatomic interaction, W-C interatomic interaction, and C-C interatomic interaction, exist. The related parameters used for MD simulation of W-C system are listed in Table 2, and the detailed descriptions of those parameters are reported in Ref.[26-27].

2 Results and Discussion

To investigate the effects of scratching depth, load, and scratching velocity on the tribological properties and crystal structure deformation of WC coating, the nano-scratching

Table 2 MD simulation parameters in Tersoff potential of W-C system

Parameter	W-W	W-C	C-C
m	1.0	1.0	1.0
γ	1.88×10^{-3}	7.2855×10^{-2}	2.0813×10^{-4}
λ_3/nm^{-1}	4.59	4.59	0.0
c	2.149 69	1.103 04	330
d	0.171 26	0.330 18	3.5
$\cos \theta_0$	0.277 8	-0.751 070	-1.1
n	1.0	1.0	1.0
β	1.0	1.0	1.0
λ_2/nm^{-1}	14.112 46	0.0	26.887 74
B/eV	306.5	0.0	1397.0
R/nm	0.35	0.28	0.185 0
D/nm	0.03	0.02	0.015
λ_1/nm^{-1}	27.195 84	0.0	32.803 05
A/eV	3401.474 4	0.0	2605.841

process is divided into two stages by a critical distance (indenter diameter): when the indenter location locates within critical distance, the process is in the transition stage (stage I); when the indenter location locates beyond the critical distance, the process is in the stable stage (stage II).

2.1 Effect of scratching depth

During the nano-scratching process of WC coating by MD simulation, the scratching depths are 0.4, 0.9, and 1.4 nm, which are the multiple values of the WC lattice constants. Fig. 3 presents MD simulations of WC-coated substrates during the nano-scratching process at different time steps under the conditions of the scratching velocity of 800 m/s, the scratching depth of 0.9 nm, and the load of 8 nN. As shown in Fig. 3, no obvious atoms are removed from the substrate at the beginning stage of the scratching process. The main reason is that the indenter contacts with the matrix, the atoms on the matrix surface are squeezed and sheared, the distance between atoms decreases, the interatomic force increases, and thereby the binding energy increases, which leads to the elastic deformation. The material deformation is directly caused by the dislocation and slip, and its deformation degree reflects the magnitude of dislocation and slip^[28]. With increasing the scratching distance, the binding energy is increased, the dislocation and slip are intensified, the plastic deformation occurs, and obvious scratching groove appears on the matrix. Some atoms break the interatomic constraints and leave the matrix surface, forming debris. The extruded atoms are accumulated in the front and both sides of the indenter. Fig. 4 shows the cross-section morphologies at the middle position along the X-direction of WC-coated substrates after scratching with different depths. It can be seen that the deformation region is mainly distributed in the surface and subsurface layer of the matrix. With increasing the scratching depth, more

substrate atoms are extruded and accumulated around the indenter, the chip atoms are increased gradually, and the groove becomes deeper.

The friction force can reflect the tribology mechanism of material during the nano-scratching process. In the nano-scratching process of WC coating, the friction force is generated by the interactions between the indenter and the substrate atoms. During the nano-scratching process, the friction force F_y and the normal force F_z of the indenter can be obtained, and the instantaneous COF (μ) can be calculated, as follows^[29]:

$$\mu = \frac{F_z}{F_y} \quad (11)$$

Fig. 5 shows the variation of scratching friction force and instantaneous COF with increasing the scratching distance. The scratching process consists of two stages. In stage I, the friction forces present a rapid increasing trend with moving forward the indenter, because the number of squeezed atoms between the indenter and the substrate is increased, and the number of interatomic interactions is also increased, as shown in Fig. 5a. When the scratching distance passes the critical location, the scratching enters into the stable stage II: the friction force and the normal force fluctuate slightly around a constant value. This is because the number of atoms between the indenter and matrix is constant. If the indenter continues to move, a lot of matrix atoms are extruded and accumulated in front of the indenter, thereby forming the wear debris. When the scratching depth is invariable, the number of interaction atoms is invariable, and the friction force and the normal force are basically stable. With increasing the scratching depth, the number of interaction atoms is increased, and the friction force and the normal force are increased.

The average friction forces and average instantaneous

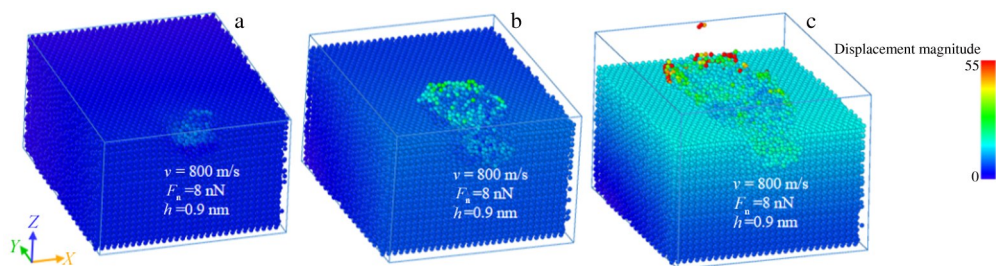


Fig.3 Atomic displacement magnitude of WC-coated substrates during nano-scratching process at time step of 2000 fs (a), 5000 fs (b), and 10 000 fs (c)

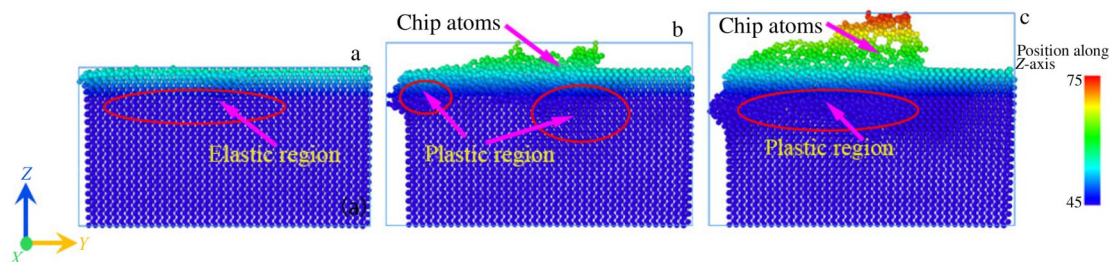


Fig.4 Atomic displacement heights of WC-coated substrates during nano-scratching process at scratching depth of 0.4 nm (a), 0.9 nm (b), and 1.4 nm (c)

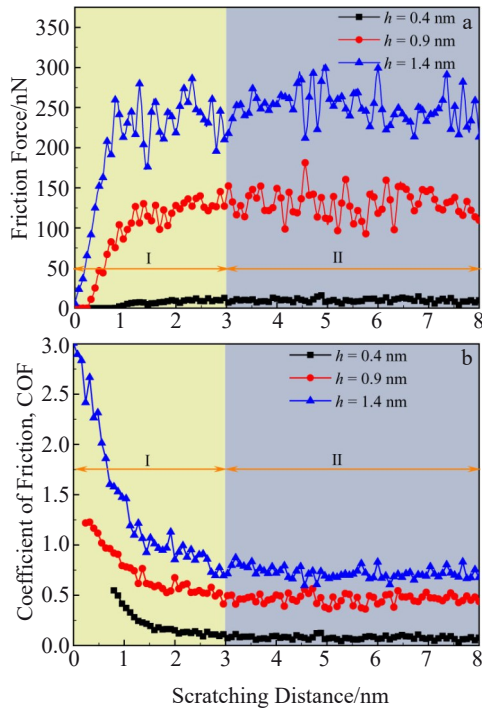


Fig.5 Friction forces (a) and COFs (b) of WC-coated substrates during nano-scratching of different depths

COFs are obtained for the further analysis of tribological performance of WC coating specimens in the stage II during nano-scratching process. Fig.6 shows the changes of average friction force and the average instantaneous COFs of WC-coated substrates during scratching of different depths. When the scratching depth is 0.4 nm and a small number of coating atoms contact with the indenter, the average friction force is close to 10 nN, and the average instantaneous COF is close to 0.08. However, when the scratching depth is 1.4 nm, a large number of coating atoms contact with the indenter, the average friction force is nearly 250 nN, and the average instantaneous COF approaches 0.72. The larger the scratching depth, the larger the contact area between the indenter and the matrix, therefore the greater the scratching hindrance force, and the greater the friction force. This result is similar to that in Ref.[30].

2.2 Effect of load

The microscopic behavior of WC coatings during nano-scratching process under different loads is revealed by the surface morphologies and the friction curves. The scratching velocity is 800 m/s, the scratching depth is 0.9 nm, and the

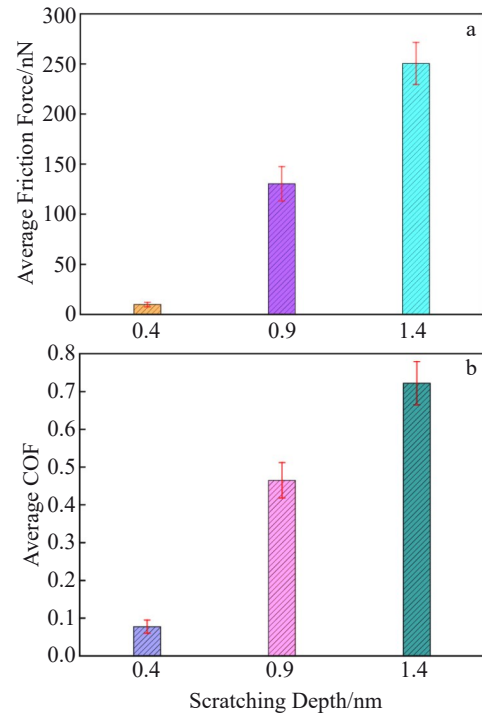


Fig.6 Average friction forces (a) and average COFs (b) of WC-coated substrates during nano-scratching of different depths

loads are 0.8, 8, and 80 nN. Fig.7 shows MD simulations of WC-coated substrates during the nano-scratching process at the scratching distance of 8 nm. The color of atoms represents different heights of atoms along Z-direction. When the load is 0.8 nN, the scratching traces are inconspicuous, because the areas at the indenter bottom are squeezed and the elastic deformation occurs. As the indenter leaves the specimen, the specimen recovers to the original state immediately. With increasing the loads, the scratching trace becomes more clear along the moving direction, and the surface crystal structure of the specimen causes damage and complex elastic-plastic deformation. In addition, with increasing the loads, the atoms are accumulated in the front and at two sides of the indenter, which gradually forms an obvious groove. The greater the load, the more the accumulated atoms in the front and at both sides of the indenter, the larger the depth and width of scratching groove, and therefore the rougher the specimen surface.

To study the friction behavior of WC-coated substrates in the nano-scratching process, the surface and cross-section morphologies under different loads are shown in Fig.8. The original matrix surfaces are marked by the black dotted lines

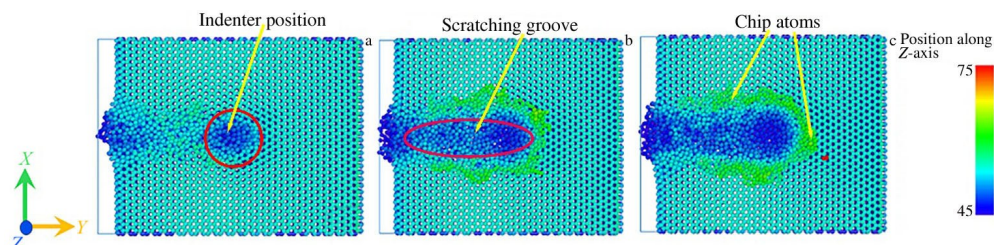


Fig.7 MD simulated deformation behavior of WC-coated substrates during nano-scratching process at load of 0.8 nN (a), 8 nN (b), and 80 nN (c)

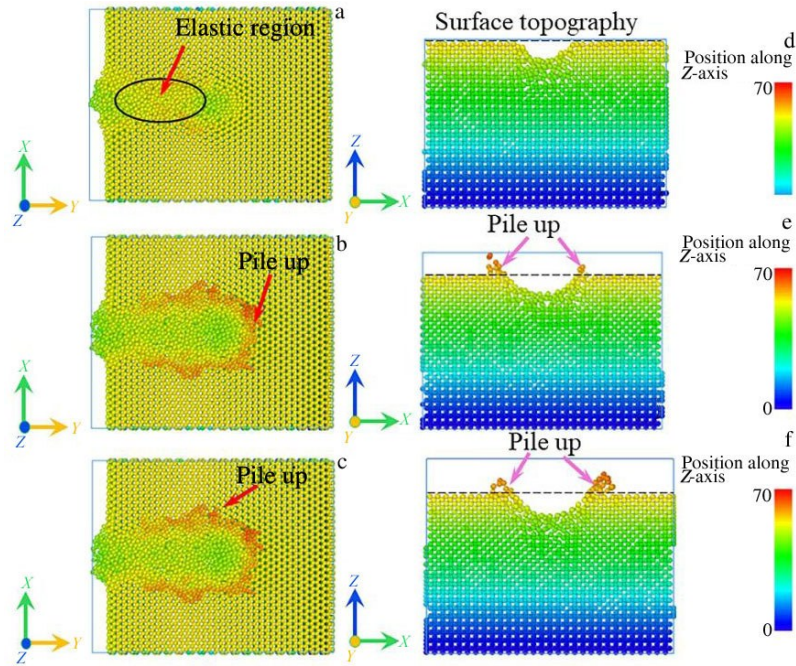


Fig.8 Surface (a–c) and cross-section (d–f) morphologies of WC-coated substrates during nano-scratching process at load of 0.8 nN (a, d), 8 nN (b, e), and 80 nN (c, f)

in Fig. 8d–8f. As shown in Fig. 8a, the elastic deformation occurs on WC-coated specimen when the load is 0.8 nN. The elastic region is indicated by the black ellipse. When the indenter leaves the specimen, the specimen atoms return to their original locations. As shown in Fig. 8d, no atoms are squeezed out from the matrix and the atoms away from the contact area are barely changed. With the scratching process proceeding, the number of atoms accumulated in the front and at both sides of the indenter is increased and the surface ploughing appears along the scratching direction, as shown in Fig. 8b. When the indenter leaves the specimen, the atoms accumulated at outer edge of the groove present a serrated distribution and they are almost symmetrically distributed along the scratch path; the atoms accumulated in the front of the indenter are still circular, as shown in Fig. 8c. These results are similar to those in Ref. [31]. According to Fig. 8e and 8f, the accumulated atoms on the matrix surface are increased and the morphology becomes rougher with increasing the loads. Additionally, the surface ploughing appears and the scratching groove becomes more wider and deeper.

Fig. 9 shows the variation of friction force and COF of WC-coated substrates during nano-scratching of different loads. In stage I, the friction force is increased with increasing the scratching distance, and then it fluctuates within a certain range in stage II. When the load is 0.8 nN, only a small number of specimen atoms have effective interactions with the indenter atoms, and the force effect on atoms is slight. Hence, the friction force is relatively small. With increasing the loads, the indenter is pressed into the matrix deeper, and the number of atoms for interaction between matrix and indenter is increased. The hindrance effect and binding energy jointly impede the motion of indenter, which inevitably increases the

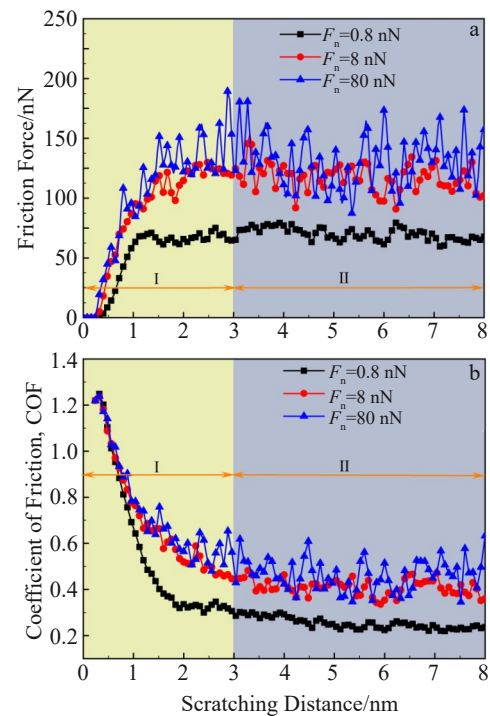


Fig.9 Friction forces (a) and COFs (b) of WC-coated substrates during nano-scratching of different loads

friction forces. This result is consistent with the results in Ref. [32]. Therefore, with increasing the load, the indenter is pressed into the matrix deeper, and the deformation and wear phenomena of WC-coated specimens become more severe.

The average friction force and the average instantaneous COF of WC-coated substrates in stage II during nano-scratching of different loads are obtained, as shown in Fig. 10.

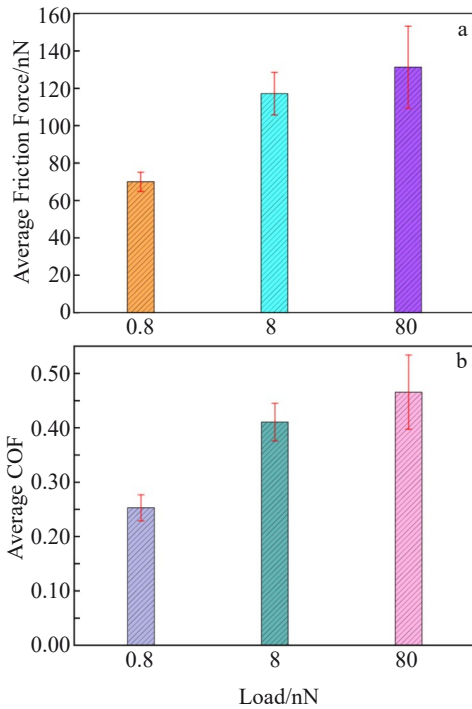


Fig.10 Average friction forces (a) and average COFs (b) of WC-coated substrates during nano-scratching of different loads in stage II

It can be found that the average friction force and average COF are increased significantly with increasing the load from 0.8 nN to 8 nN. This is because the bottom zone of the indenter undergoes elastic deformation under low load. When the load increases, these zones undergo plastic deformation and suffer from crystal structure damage, resulting in rapid increase in average friction force and average instantaneous COF. According to Fig.10, the average friction force and the average COF is 47 nN and 0.16 when the load is 8 nN, respectively; when the load is 80 nN, the average friction force and the average COF increases to 14 nN and 0.50, respectively. With increasing the load, the nano-scratching process become more complicated.

2.3 Effect of scratching velocity

The effect of scratching velocity on the friction behavior of WC-coated substrates in nano-scratching process was also investigated. The scratching velocity is 200, 400, and 800 m/s,

the scratching depth is 0.9 nm, and the load is 16 nN. Fig.11 shows MD simulations of WC-coated substrates during scratching process at different scratching velocities. The color of atoms represents different heights of atoms along Z-direction. The wear morphologies of WC-coated substrates are obtained at different scratching velocities. The results show that the matrix atoms are accumulated and arranged more closely with increasing the scratching velocity under the same load and scratching distance. The wear debris is symmetrically accumulated on both sides of the scratching groove. The accumulated atoms on the outer edge are smooth under low velocity, as shown in Fig. 11a. The scratching groove becomes wider and the outer edges on the surface present burrs at the velocity of 400 m/s, as shown in Fig. 11b. The specimen atoms are squeezed by the indenter, which cannot be dispersed to both sides. Particularly at high velocity, the specimen atoms move forward and are gradually accumulated in front of the indenter. The number of accumulated atoms becomes more and more with increasing the scratching velocity, the atom position along the Z-direction becomes higher, and the surface becomes rougher, as shown in Fig.11c.

Zhu et al.^[33] found that if the atom displacement is greater than threshold height, the atom can be deemed as wear debris atom during the nano-scratching process. The threshold height is usually considered as the half length of the lattice constant of material. Fig. 12 shows the morphologies of wear debris atoms on WC-coated substrates during nano-scratching process at different scratching velocities and fixed scratching depth and load. The color of atoms represents different heights of atoms along Z-direction. As shown in Fig. 12a, the wear debris atoms are distributed on both sides and in the front of the scratching groove, and the accumulated atoms are symmetrically distributed along the scratching orientation at velocity of 200 m/s. According to Fig. 12b, the quantity and displacement of wear debris atoms distributed on both sides of the scratching groove are increased significantly with increasing the scratching velocity from 200 m/s to 400m/s. As shown in Fig. 12c, it is found that the wear debris atoms on the surface present serrated and asymmetrical distributions, the position of accumulated debris atoms in Z-direction is higher, and the surface is rougher at scratching velocity of 800 m/s. These results are similar to those in Ref.[34–35].

Center symmetric parameters (CSPs) are important

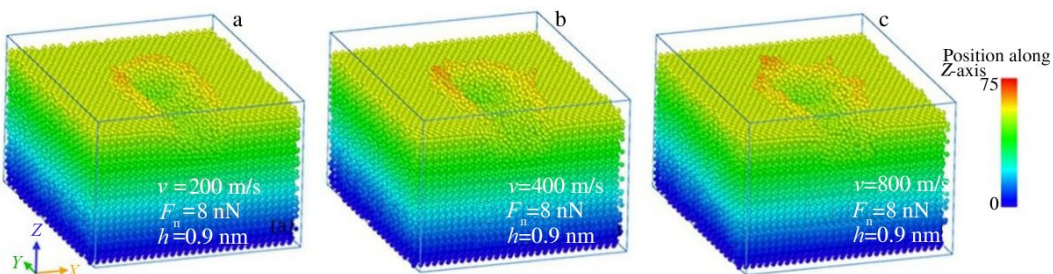


Fig.11 Deformation behavior of WC-coated substrates during nano-scratching process at scratching velocity of 200 m/s (a), 400 m/s (b), and 800 m/s (c)

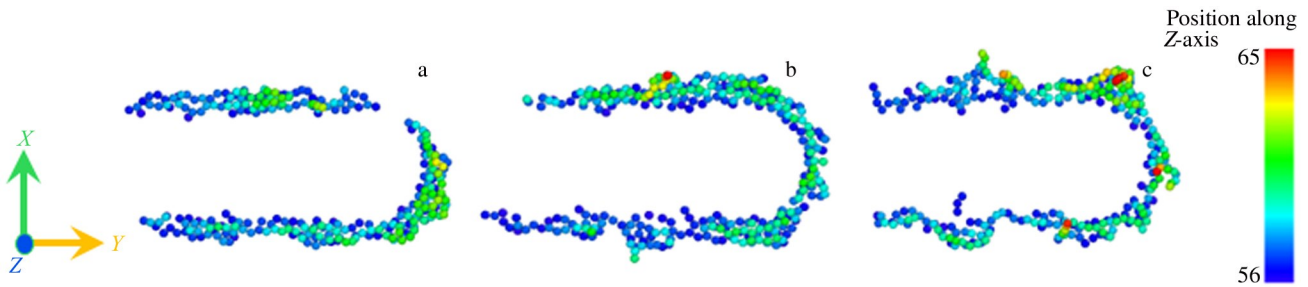


Fig. 12 Wear debris atom morphologies on WC-coated substrates during nano-scratching process at scratching velocity of 200 m/s (a), 400 m/s (b), and 800 m/s (c)

parameters to analyze the dislocation, defect, and stratification in crystalline materials, and they can directly indicate the disorder degree of crystal atoms^[36]. As for the perfect crystal materials, CSP value approaches to 0. The larger the CSP value, the higher the asymmetry degree. CSP method was used in this research to investigate the dislocation slip and defect structure of the WC coating model during nano-scratching under different scratching velocities. It is revealed that the specimen undergoes elastic-plastic deformation due to the mixed actions of extrusion, tension, and shear of the indenter. According to Fig. 13, some damaged layers exist beneath the scratching groove and the defect structures of the specimen appear on surface and subsurface in the nano-scratching process. CSP value of debris atoms becomes larger and the defect atoms in matrix are relatively small. The dislocation nucleation and emission inside the matrix lead to the formation of defect layer. The main defect structures formed in the nano-scratching process are interstitial, vacancy atoms, atomic clusters, stair-rod dislocation, and V-shape dislocation. The atomic clusters are mainly distributed below the scratching, the stair-rod dislocation is located under the scratching groove and indenter, and the V-shape dislocation appears below the indenter. Under different scratching velocities, the depth of defect layers and the defect structures beneath the indenter are greatly changed. As a result, the higher the scratching velocity, the deeper the defect layer.

As shown in Fig. 14a, it is revealed that the scratching velocity results in slight difference in the friction force in stage I, and the friction force in stage II fluctuates obviously at high scratching velocity, compared with that at low scratching velocity. The scratching process causes the stress-strain in the indenter contact region, which leads to the atom

nucleation and dislocations of the matrix. Under high velocities, the dislocations do not have sufficient time to slip from the contact region and to release the concentration stress, which causes the atom slip along scratching orientation. The atom accumulation in front of the indenter hinders the indenter motion. Based on the computational results, the higher the scratching velocity, the more the dislocations, thereby the larger the strain rate, and the less the time for dislocation slip, which causes the fluctuation and increase of friction force. The similar phenomenon is also reported in Ref. [37]. Fig. 14b presents the average instantaneous COF of WC-coated substrates during nano-scratching of different scratching velocities. The instantaneous COF dramatically decreases in the stage I, and it reaches a stable value in stage II. This is because the number of interaction atoms along normal direction dramatically increases when the indenter contacts with the matrix, which leads to a larger increment in the normal force, compared with that in friction force. When the nano-scratching process enters a stable stage, the number of interaction atoms is stable and the average instantaneous COF slightly fluctuates near the equilibrium value.

In order to investigate the general tribological performance of WC-coated substrate, the average friction forces and average COFs of WC-coated substrates in stage II during nano-scratching process of different scratching velocities are studied. As shown in Fig. 15, the average friction force and average COF are increased with increasing the scratching velocity. The average friction force and instantaneous COF are slightly affected by the variation of velocity. When the scratching velocity increases from 200 m/s to 400 m/s, the average friction force increases by 2 nN, and the average instantaneous COF increases by 0.028. When the scratching

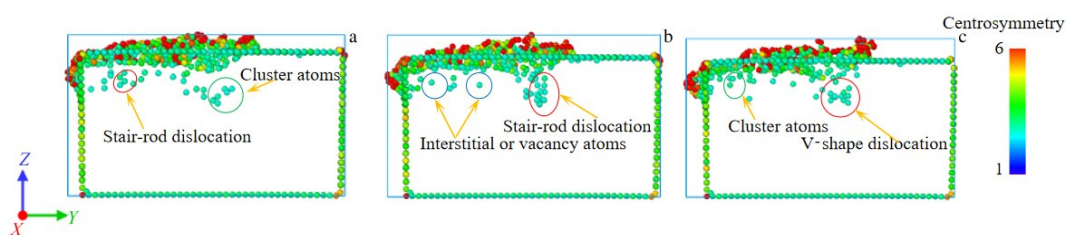


Fig. 13 Crystal structure defects in WC-coated substrates during nano-scratching process at scratching velocity of 200 m/s (a), 400 m/s (b), and 800 m/s (c)

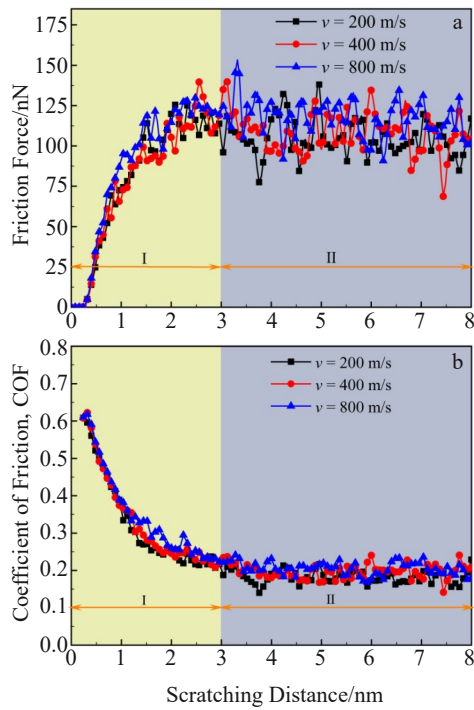


Fig.14 Friction forces (a) and COFs (b) of WC-coated substrates during nano-scratching of different scratching velocities

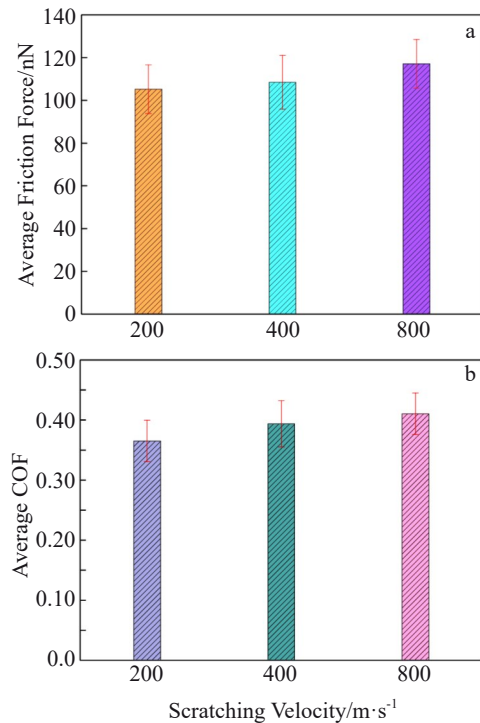


Fig.15 Average friction forces (a) and average COFs (b) of WC-coated substrates during nano-scratching of different scratching velocities

velocity increases from 400 m/s to 800 m/s, the friction force increases by 9 nN, and the average instantaneous COF increases by 0.017.

3 Conclusions

1) In the nano-scratching process, the scratching depth is a critical parameter for nano-friction properties of WC coating. The deeper the scratching depth, the more severe the elastoplastic damage, the more the accumulated atoms, and the rougher the friction surface. Particularly, when the scratching depth exceeds the lattice constant, the surface morphology becomes rougher, the scratching groove becomes deeper, and the wear debris increases.

2) The loads play an important role in the crystal structure change in the nano-friction process of WC coating. The load causes the crystal dislocation and slip, which leads to the elastic deformation and plastic deformation beneath the contact region. With increasing the load, the nano-scratching process become more complicated.

3) The scratching velocity has great effect on the surface morphology and wear debris distribution of WC-coated substrate. The higher the scratching velocity, the deeper the defect layer, the higher the position of accumulated atoms along the scratching direction, and the worse the symmetrical distribution of wear atoms on both sides of scratching groove.

4) This research is conducted based on the molecular dynamics method, which agrees well with the experiment results in other references, providing critical supplement to understand the tribological properties of WC coating at nano-scale.

References

- 1 Ali E, Ramirez G, Osman L E et al. *Nature*[J], 2016, 536(7614): 67
- 2 Sandra C, Thibault C, Francois O. M et al. *ACS Applied Materials & Interfaces*[J], 2016, 8(6): 4208
- 3 Song Z L, Tang X, Chen X et al. *Thin Solid Films*[J], 2021, 736: 138 906
- 4 Akihiro K, Kaito T, Masayuki A. *Surface & Coatings Technology*[J], 2020, 394: 125 881
- 5 Sabea H A, Taher R, Neda F N. *Protection of Metals and Physical Chemistry of Surfaces*[J], 2019, 55(5): 936
- 6 Sun Z, Zhu S G, Dong W W et al. *Ceramics International*[J], 2021, 47: 16 441
- 7 Xiao Q, Sun W L, Yang K X et al. *Surface & Coatings Technology*[J], 2021, 420: 127 341
- 8 Marek B, Annamária D, Tamás C et al. *Journal of the European Ceramic Society*[J], 2014, 34(14): 3407
- 9 Roebuck B, Moseley S. *International Journal of Refractory Metals and Hard Materials*[J], 2015, 48: 126
- 10 Tarragó J M, Roa J, Jiménez-Piqué E et al. *International Journal of Refractory Metals and Hard Materials*[J], 2016, 54: 70
- 11 Saeed Z C, Xu S Z. *Progress in Materials Science*[J], 2019, 100: 1
- 12 Yang Shengze, Cao Hui, Liu Yang et al. *Rare Metal Materials and Engineering*[J], 2022, 51(9): 3236 (in Chinese)

- 13 Isha S, Ankit K, Subrata K G et al. *Journal of Molecular Liquids*[J], 2021, 335: 116 154
- 14 Anil B S, Shivanjali P, Pooja P et al. *Materials Today: Proceedings*[J], 2021, 49: 1453
- 15 Singh R, Sharma V. *Computer Material Science*[J], 2021, 197: 110 653
- 16 Xu Y M, Zhu P Z, Li R et al. *Molecular Simulation*[J], 2022, 48(12): 1072
- 17 Feng Q, Song X Y, Xie H X et al. *Materials and Design*[J], 2017, 120: 193
- 18 Guo J, Chen J J, Lin Y Z et al. *Applied Surface Science*[J], 2021, 539: 148 277
- 19 Hua D P, Wang W, Luo D W et al. *Journal of Materials Science & Technology*[J], 2022, 105: 226
- 20 Aidan P T, Aktulga H M, Berger R et al. *Computer Physics Communications*[J], 2022, 271: 108 171
- 21 Stukowski A. *Modelling and Simulation in Materials Science and Engineering*[J], 2010, 18: 15 012
- 22 Guo Y J, Yang X J, Qin S Y et al. *Rare Metal Materials and Engineering*[J], 2022, 51(2): 436
- 23 Lan H Q, Xu C. *Acta Physica Sinica*[J], 2012, 61(13): 133 101
- 24 Hui Z X, He P F, Dai Y et al. *Acta Physica Sinica*[J], 2014, 63(7): 74 401
- 25 Tersoff J. *Physical Review B*[J], 1989, 39(8): 5566
- 26 Juslin N, Erhart P, Träskelin P et al. *Journal of Applied Physics*[J], 2005, 98: 123 520
- 27 Petisme M V G, Gren M A, Wahnström G. *International Journal of Refractory Metals and Hard Materials*[J], 2015, 49: 75
- 28 Guo X G, Gou Y J, Dong Z G et al. *Applied Surface Science*[J], 2020, 56: 146 608
- 29 Zhang C, Farhat Z N. *Wear*[J], 2009, 267: 394
- 30 Alidokht S A, Chromik R R. *Wear*[J], 2021, 477: 203 792
- 31 Gao Y, Brodyanski A, Kopnarski M et al. *Computational Materials Science*[J], 2015, 103: 77
- 32 Xie H C, Ma Z C, Zhao H W et al. *Materials Today Communications*[J], 2022, 30: 103 072
- 33 Zhu P Z, Hu Y Z, Ma T B et al. *Tribology Letters*[J], 2011, 41(1): 41
- 34 Liu X M, Liu Z L, Wei Y G. *Computational Materials Science*[J], 2015, 110: 54
- 35 Zhu J X, Xiong C B, Ma L et al. *Tribology International*[J], 2020, 150: 106 385
- 36 Liang Y, Wang Q, Yu N et al. *Nanoscience and Nanotechnology Letters*[J], 2013, 5(5): 536
- 37 Tian Y Y, Li J, Luo G J et al. *Tribology International*[J], 2022, 169: 107 435

WC 涂层纳米划痕过程中摩擦学性能及演化特征的分子动力学研究

罗宏博¹, 吕延军¹, 赵晓伟¹, 张永芳²

(1. 西安理工大学 机械与精密仪器工程学院, 陕西 西安 710048)

(2. 西安理工大学 印刷包装与数字媒体学院, 陕西 西安 710048)

摘要: 为研究纳米划擦过程中 WC 涂层纳米级摩擦演化特征, 利用大型原子/分子大规模并行模拟器建立了不同条件 (载荷、划痕深度、划痕速度) 下的分子动力学模拟模型。结果表明: 摩擦力和摩擦系数随着划痕深度的增加而增大; 当压头划擦试样时, 沿划痕方向在压头前方及凹槽两侧的原子被挤压、剪切、堆积。瞬时摩擦曲线在初始阶段和稳定阶段表现出明显的摩擦学特征, 摩擦过程中压头下方区域晶体出现错位、滑移、间隙或空位。随着划痕速度的增加, 体系应变能超过原子间相互约束, 原子突破约束, 在划痕沟槽两侧堆积, 堆积的表面形貌和外缘变得粗糙, 亚表面晶体结构产生缺陷。本研究有助于在纳米尺度了解 WC 涂层摩擦过程的微观磨损机理。

关键词: WC 涂层; 纳米划擦; 分子动力学模拟; 摩擦力; 摩擦系数; 形貌

作者简介: 罗宏博, 男, 1984 年生, 博士生, 西安理工大学机械与精密仪器工程学院, 陕西 西安 710048, E-mail: 1190211020@stu.xaut.edu.cn